

Stress–strain behavior of cement-improved clays: testing and modeling

Allison J. Quiroga¹  · Zachary M. Thompson² ·
Kanthasamy K. Muraleetharan¹ · Gerald A. Miller¹ ·
Amy B. Cerato¹

Received: 18 July 2016 / Accepted: 13 February 2017 / Published online: 10 March 2017
© Springer-Verlag Berlin Heidelberg 2017

Abstract The results of a series of laboratory tests on unimproved and cement-improved specimens of two clays are presented, and the ability of a bounding surface elastoplastic constitutive model to predict the observed behavior is investigated. The results of the oedometer, triaxial compression, extension, and cyclic shear tests demonstrated that the unimproved soil behavior is similar to that of soft clays. Cement-improved specimens exhibited peak/residual behavior and dilation, as well as higher strength and stiffness over unimproved samples in triaxial compression. Two methods of accounting for the artificial overconsolidation effect created by cement improvement are detailed. The apparent preconsolidation pressure method is considerably easier to use, but the fitted OCR method gave better results over varied levels of confining stresses. While the bounding surface model predicted the monotonic behavior of unimproved soil very well, the predictions made for cyclic behavior and for improved soils were only of limited success.

Keywords Cemented clay · Cement-improved clay · Chemical stabilization · Constitutive model · Triaxial testing

List of symbols

A_c	Shape parameter defining hyperbola section of bounding surface in compression
A_e	Shape parameter defining hyperbola section of bounding surface in extension
a_w	Cement content
C	Projection center parameter
C_c	Virgin compression index
C_r	Recompression index
C_C	Coefficient of curvature
C_U	Coefficient of uniformity
D_{50}	Diameter in the grain size distribution curve corresponding to 50% passing
e	Void ratio
h_2	Shape hardening parameter for states in immediate vicinity of I axis
h_c	Shape hardening parameter in triaxial compression
h_e	Shape hardening parameter in triaxial extension
M_c	Slope of the critical state line in compression
M_e	Slope of the critical state line in extension
p'	Mean effective stress
q	Deviatoric stress
q_n	Normalized deviatoric stress
R_c	Shape parameter defining ellipse 1 section of bounding surface in compression
R_e	Shape parameter defining ellipse 1 section of bounding surface in extension
S	Elastic nucleus parameter
S_g	Specific gravity
T	Shape parameter defining ellipse 2 section of bounding surface
u	Excess pore water pressure
u_n	Normalized excess pore water pressure
V_{soil}	Volume of soil solids

✉ Allison J. Quiroga
quir5964@ou.edu

¹ School of Civil Engineering and Environmental Science, University of Oklahoma, 202 W. Boyd Street, Room 334, Norman, OK 73019-1024, USA

² ONEOK, ONEOK Plaza 100 West 5th Street, Tulsa, OK 74103, USA

W_c	Mass of cement
W_s	Mass of soil solids
$W_{w,mix}$	Mass of water in total improved soil sample
$W_{w,slurry}$	Mass of water in slurry
$w:c$	Water-to-cement ratio
$w_T:c$	Total water-to-cement ratio
α	Cement factor
ε_a	Axial strain
κ	Slope of the recompression line in e versus $\ln(p')$ space
λ	Slope of the virgin compression line in e versus $\ln(p')$ space
ν	Poisson's ratio
σ_b	Back pressure
σ'_1	Effective axial stress
σ'_3	Effective confining stress
σ'_c	Effective consolidation stress
σ'_p	Effective preconsolidation pressure
σ'_v	Effective vertical stress

Terms

Apparent preconsolidation pressure	The yield stress determined from improved specimen oedometer test results
Fitted overconsolidation ratio (OCR)	The OCR value calibrated using test results by treating it as a constitutive model parameter
Imposed OCR	The OCR calculated from the maximum confining stress imposed during the consolidation phase and the confining stress prior to the start of the shear phase in a triaxial test

1 Background

Since the 1970s, researchers and designers have been using deep mixing chemical soil stabilization methods for various applications in civil engineering practice [3, 43]. Generally, the purposes of chemical improvement include increasing the strength and stiffness of a marginal soil or decreasing the permeability of a loose soil [37]. Deep mixing methods allow chemical stabilization to be completed at large depths below the ground surface [37]. In practice, such improvement methods have been used to increase the bearing capacity of foundations, decrease settlements, reinforce slopes and excavations, and control seepage in dams and contaminated sites, among other applications [37].

Much research has been dedicated to characterizing the engineering properties of these chemically treated soils and developing design tools and guidelines for practitioners [8, 52]. Use of cement as the stabilizing agent creates cementitious and pozzolanic bonds between soil particles. The engineering behavior of cement-improved clays has been shown to be influenced by a number of factors such as the initial soil type, cement content, water-to-cement ratio, and curing time [21, 36, 44]. One-dimensional compression curves for improved clays show a large amount of non-linearity; however, zones similar to recompression and virgin compression zones, as well as a yield stress, often referred to as the apparent preconsolidation pressure, can still be identified [2, 17, 31, 54]. In other words, cement improvement seems to create an artificial overconsolidation effect in clays. Results of triaxial compression tests on improved specimens have also demonstrated artificial stress histories, which depend on both cement content and confining stress [2, 23, 59]. These tests showed behaviors ranging from those similar to heavily overconsolidated clays for improved specimens with high cement contents or low confining stresses to lightly overconsolidated clays for improved specimens with low cement contents or high confining stresses [59]. Limited triaxial extension and cyclic test results on improved clays exist in the literature. The most significant contributions in this area have been related to the cyclic characteristics used for roadway applications [1, 35, 57]. Upadhyaya et al. [55] published results for cyclic shear tests on improved clays with large shear strains. Recognizing that bonded soils exhibited unique stress–strain behaviors, researchers started to propose constitutive models for naturally bonded soils [e.g., 6, 7, 19, 24, 34, 41, 51] in the early 2000s. This class of models was then extended to include models better suited to artificially cemented soils [e.g., 4, 5, 12, 14, 18, 22, 27, 33, 45, 46, 56, 58]. Although the exact methods vary, each model determines the size of the yield surface using some bond parameter which, in most cases, decreases due to loading or accumulated strain.

The use of cement-improved clays in seismic regions is increasing [38]. One application of cement improvement in soft clay profiles is to decrease the potential for large lateral deflections of piles and pile groups by strengthening the surficial soils surrounding the piles using a technique called cement deep soil mixing (CDSM). The Network for Earthquake Engineering Simulation-piles in low E soils (NEES-pilEs) project aims to characterize the seismic behavior of and provide guidance on the design of such systems through a two-pronged approach of testing and computational modeling. As a part of this project, several centrifuge tests [25, 26, 28, 29, 48–50] and a full-scale field test [11] were performed. Computational modeling is being used to expand the data on behavior of pile systems in

CDSM reinforced soil beyond those configurations and loading histories which were directly tested through the centrifuge and field tests. One such computer code that is being used in this study is TeraDysac [32, 40]. TeraDysac is a three-dimensional, fully coupled finite element code capable of simulating static and dynamic problems in saturated and unsaturated soils, including soil–structure interaction problems. To date, no constitutive model for the prediction of soil–cement stress–strain behavior has been implemented into the TeraDysac platform. Of the constitutive models currently available within TeraDysac, the bounding surface elastoplastic model [9] was deemed to be the most appropriate choice to simulate cement-improved clay. Kirupakaran et al. [20] presented an initial investigation of using TeraDysac, and the bounding surface model, to simulate the behavior of improved pile systems subject to base shaking.

The two clay soils investigated in this study are the laboratory-created soil used in centrifuge tests, and the natural clay found at the field site in Miami, Oklahoma. Laboratory test results, including triaxial cyclic and extension test results, for the laboratory-created [53] and the natural clay [39] are presented and analyzed in this paper. The ability of the bounding surface plasticity model [9] to predict the stress–strain behavior of improved and unimproved clays is also investigated in this paper. Two methods of accounting for the artificial stress history resulting from cement improvement are proposed. The laboratory testing and modeling results presented herein will aid researchers interested in computationally simulating the above-mentioned centrifuge and field tests. In fact, Taghavi [50] used the unimproved and improved (with fitted OCR method) laboratory-created clay model parameters presented in this paper within TeraDysac to simulate a centrifuge test of pile groups in unimproved and improved soft clays subject to base shaking. Taghavi's predictions showed reasonable agreement with centrifuge test results, indicating that the level of accuracy in single element constitutive model predictions discussed in subsequent sections may be sufficient to predict the macroscale behavior in boundary value problems, especially at small to moderate stresses far from failure.

2 Specimen creation and laboratory testing

Two clay soils were used in this study, both in unimproved and cement-improved states. A series of oedometer and triaxial tests, including isotropically consolidated undrained compression (CIUC), extension (CIUE), and cyclic (CIU Cyclic) loading, were completed for each soil type.

2.1 Choice of soils and soil properties

The characterization and soil testing presented in this study were completed to aid in centrifuge and field testing performed during the NEES-pilEs project. The clay used in centrifuge testing is a laboratory-created soil. Three requirements were imposed in the mix design for this soil: (1) that the soil be classified as a clay by all common soil classification systems, (2) that the soil properties and specimen behavior remain consistent between all samples, and (3) that consolidation be made efficient, with respect to time, by creating a clay with relatively high permeability [53].

Specimens were created using the slurry consolidation method described by Sheeran and Krizek [42]. The clay was created by mixing a commercially available (No. 1 Glaze Clay from Old Hickory Clay Company in Hickory, Kentucky) kaolin (70.8% kaolinite, 22.4% quartz, 4.5% feldspar, 2.3% miscellaneous trace minerals) and a fine sand ($S_g = 2.65$, $D_{50} = 0.14$ mm, $C_U = 1.6$, $C_C = 1$) from George Townsend Co., Inc. in Oklahoma City, Oklahoma (Quikrete Commercial Grade Fine White Sand, No. 1961-55). The slurry consisted of 1:1 kaolin/sand by dry weight mixed at a water content of 64% (twice the Liquid Limit). The slurry was placed into a consolidation device depicted in Fig. 1. Axial loads were incrementally applied, and the vertical deformation of the soil column was recorded. The final load increment imposed a vertical stress of approximately 103 kPa, the average overburden pressure in the clay layer during centrifuge testing. After consolidation, the soil was extruded from the consolidation device for testing.

The natural clay in this study was retrieved from the field test site in Miami, Oklahoma. This site has a 3.4-m layer of medium stiff to very soft silty clay underlying a top layer of lean clay with gravel and construction debris. Undisturbed soil samples were taken from 0.5 to 4.0 m below the ground surface [47]. Initial testing showed the clay layer to be homogeneous along the full depth, and therefore, the results from multiple depths are combined together in the analyses of the results. Some of the key soil properties of both the laboratory-created and natural clays are summarized in Table 1. Although Liquid Limit, Plastic Limit, and average water content are similar for both the soils, the natural soil has more fines.

Improved clay specimens were created using both clay soils. The mix design properties for both soils are listed in Table 2. Water-to-binder ratio ($w:c$), binder content (a_w), binder factor (α), and total water-to-binder ratio ($w_T:c$) are standard measures used in chemical soil improvement, proposed by Filz et al. [10]. As cement is the binder used in this research, the term 'binder' was replaced with 'cement' for clarity. The pertinent definitions are as follows:

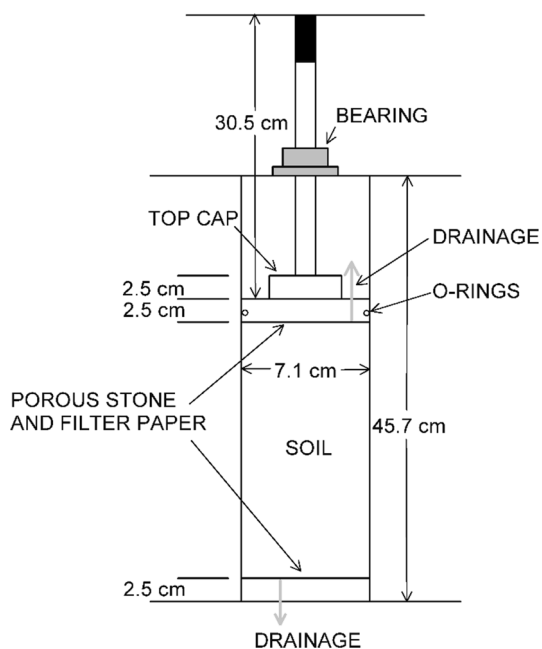


Fig. 1 Slurry consolidation device

Table 1 Soil properties of tested clays

	Laboratory-created clay	Natural clay
USCS classification	CL	CL
Liquid limit (%)	32	31
Plastic limit (%)	17	18
Average water content (%)	28.4	29.6
Percent passing #200 sieve (%)	50	93.3
Specific gravity	2.69	2.76

$$w:c = \frac{W_{w,slurry}}{W_c} \quad (1)$$

$$a_w = \frac{W_c}{W_s} \times 100\% \quad (2)$$

$$\alpha = \frac{W_c}{V_{soil}} \quad (3)$$

$$w_T:c = \frac{W_{w,mix}}{W_c} \quad (4)$$

The mix design used in this study for both the laboratory-created and natural clays aimed to recreate the amount of cementation and water-to-cement ratios used in the centrifuge and field tests, respectively. In both cases, prospective mix designs were investigated with a series of unconfined compression tests (UCT) in accordance with ASTM D2166. Figure 2 shows the increase in unconfined compression strength (UCS) with curing time and cement content ($w:c = 1$). The final cement contents selected were

Table 2 Mix design properties of improved clay specimens

	Laboratory-created clay	Natural clay
Water-to-cement ratio	1	1
Cement content (%)	10	20
Cement factor (kg/m^3)	270	550
Total water-to-cement ratio	4.40	2.48
Curing time (days)	28	60

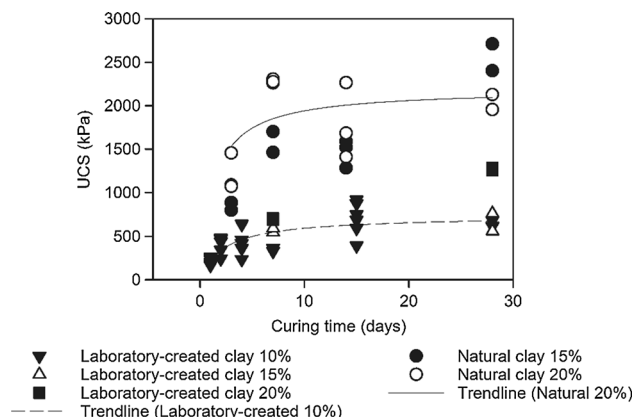


Fig. 2 Unconfined compression strength with curing time and cement content

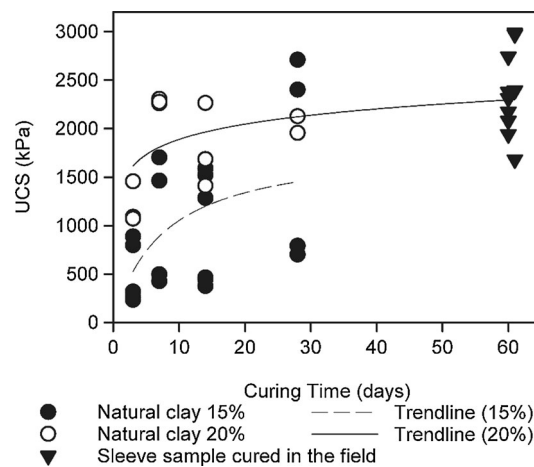


Fig. 3 Unconfined compression strength of improved natural clay

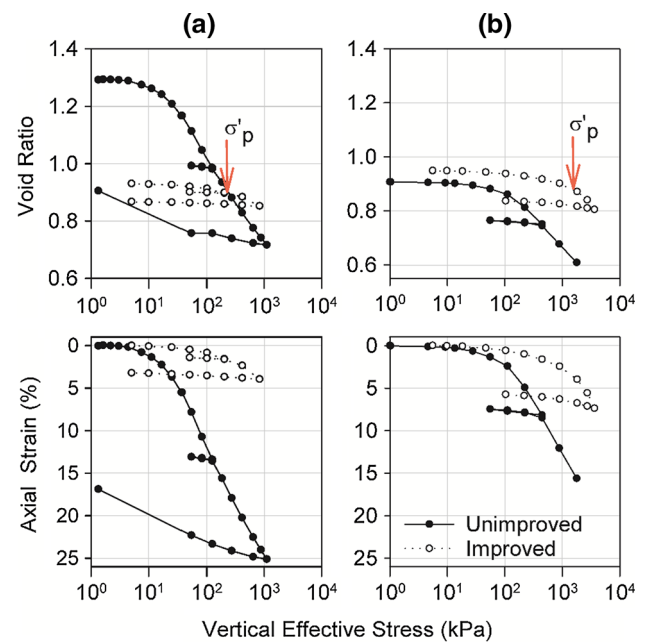
10 and 20% for the laboratory-created and natural clays, respectively. In Fig. 3, the variation of UCS with curing time and cement content is shown for the natural clay. Also shown in this figure are the UCS values for the samples taken from a special double sleeve sampler installed in the field and retrieved after 60 days of curing during the pile testing. Note that 60 days of field curing resulted due to schedule constraints for the pile testing. The trend lines indicate the logarithmic best fit for the laboratory-improved specimens

Table 3 Saturation and consolidation details for triaxial tests

Soil type	Test designation		Consolidation	
	Test type	Imposed OCR	Max σ'_c (kPa)	Final σ'_c (kPa)
Laboratory-created clay				
Unimproved	CIUC	1.0	207	207
	CIUC	1.2	207	179
	CIUC	9.0	345	38
	CIUE	1.0	207	207
	CIUE	4.4	207	47
	Cyclic	1.0	207	207
Improved	CIUC	1.0	207	207
	CIUC	1.5	207	138
	CIUC	5.0	207	41
	CIUE	1.0	207	207
	CIUE	5.0	207	41
	Cyclic	1.0	207	207
Natural clay				
Unimproved	CIUC	1.0	207	207
	CIUC	2.0	207	103
	CIUC	5.0	207	41
	CIUE	1.0	207	207
	CIUE	4.43	214	48
	Cyclic	1.0	207	207
Improved	CIUC	1.0	207	207
	CIUC	1.83	219	120
	CIUC	5.0	207	41
	Cyclic	1.0	207	207

of various cement contents. The 20% cement content trend line is extended to show a prediction for 60 days UCS. Although the factors which control the increase in strength due to cement improvement in the field are varied and complex, Fig. 3 shows the mix design used in laboratory-improved natural clay samples is a good representation of the approximately 20% cement content and 1:1 water-to-cement ratio used during improvement in the field [11].

Mixing procedures for laboratory improvement were similar to those outlined by Hodges et al. [13], Filz et al. [10], and the Japanese Geotechnical Society [15]. The laboratory clay was first created with an initial water content of 34% (the average water content of the clay layer in centrifuge tests after consolidation) before the addition of the cement slurry. For the natural clay, previously tested unimproved natural clay triaxial specimens were combined and mixed to a water content of 29.6%, the average in situ water content from the Shelby tube specimens, before being mixed with the cement slurry. For both natural and laboratory-created clays, the unimproved soil was mixed with cement–water slurry by hand. The improved clay

**Fig. 4** Oedometer test results: **a** laboratory-created clay; **b** natural clay

mixture was placed into cylindrical molds and tamped to minimize air voids. Mass was used as an indicator to ensure consistency in void ratio among samples. Specimens were removed from the molds after 1 day and cured in a temperature and humidity-controlled room. The laboratory-created and natural clay specimens were cured 28 and 60 days, the amount of time the improved soils were allowed to cure for the centrifuge and field tests, respectively. For oedometer testing, the tests began on the last day of curing. For triaxial tests, the tests were scheduled in order to allow shearing of the sample to occur on the final day of curing.

2.2 Testing protocol

Each specimen type was subjected to a similar laboratory testing regimen of one-dimensional consolidation and triaxial testing. Oedometer specimens were saturated during the initial loading increments of each test. The soil volume was allowed to change freely due to the addition of water. Limitations of the testing apparatus dictated the maximum vertical stress applied during these tests. Triaxial testing included isotropically consolidated undrained compression (CIUC), extension (CIUE), and cyclic (CIU Cyclic) tests. Samples were first back pressure saturated. During the consolidation phase of testing, various overconsolidation ratios (OCRs) were imposed through loading and unloading of the specimens. Stresses imposed for improved soil consolidation were chosen to mirror the OCRs used in the corresponding unimproved specimen testing. These

Table 4 Compression indices

	Laboratory-created clay		Natural clay	
	Unimproved	Improved	Unimproved	Improved
Virgin compression index	0.322	0.104	0.240	0.285
Recompression index	0.067	0.006	0.016	0.015
Preconsolidation stress (kPa)	25	225	130	1500

imposed OCRs represent the history of stresses applied to the specimens, not any artificial OCR that resulted from cement improvement. A complete list of the triaxial test results presented in this paper with test details is given in Table 3.

Compression shear tests were run with a constant axial strain rate of 1% per hour for unimproved specimens and 4% per hour for improved specimens. These rates were

chosen in accordance with ASTM D4767 and oedometer test results. Two extension shear procedures were used during testing: strain-controlled tests in which the axial stresses decreased while the cell pressure remained constant and stress-controlled tests in which the cell pressure was increased while the axial stress remained constant. Limits on the testing apparatus did not allow for successful completion of CIUE testing on improved natural

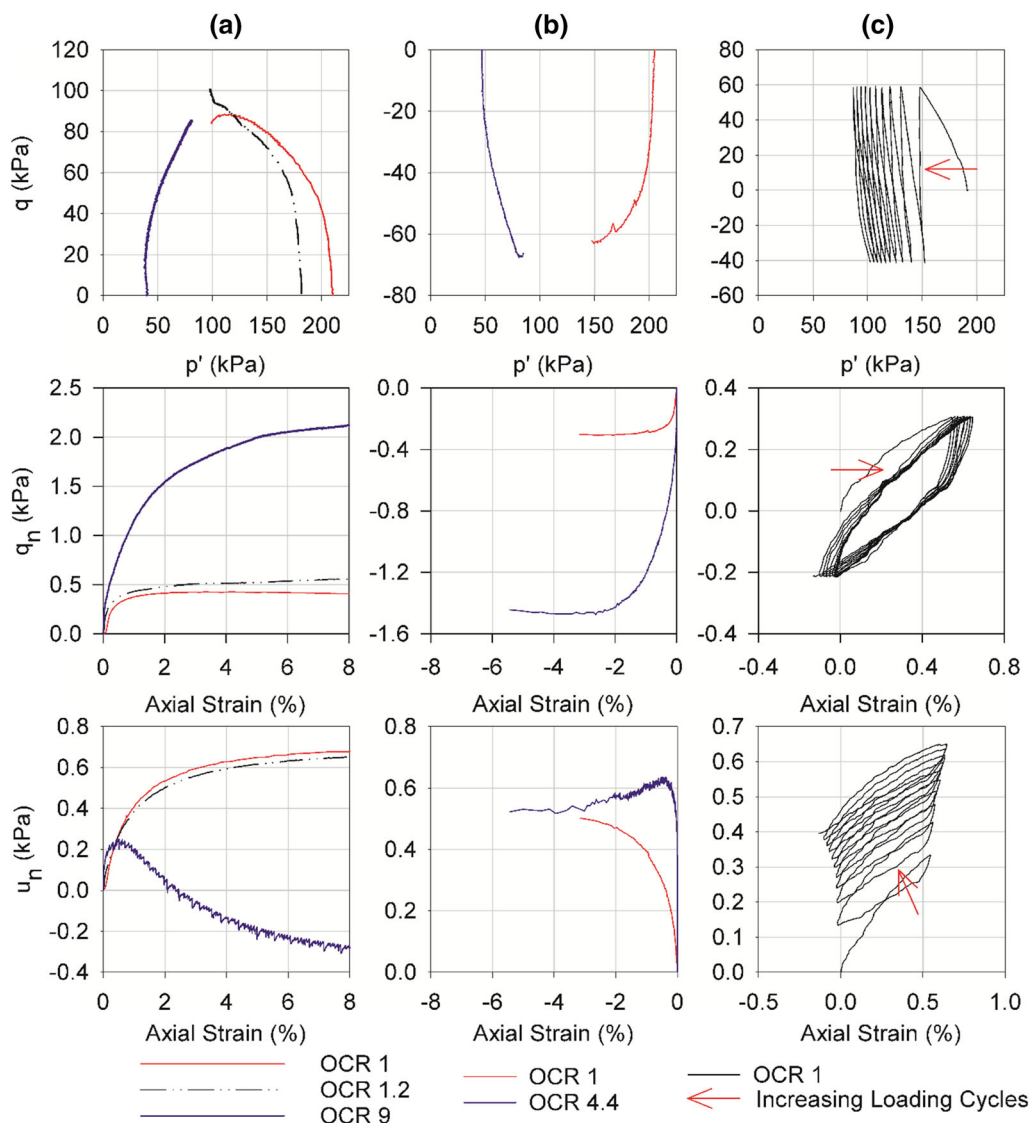


Fig. 5 Triaxial test results for unimproved laboratory-created clay: **a** CIUC tests; **b** CIUE tests; **c** CIU Cyclic test

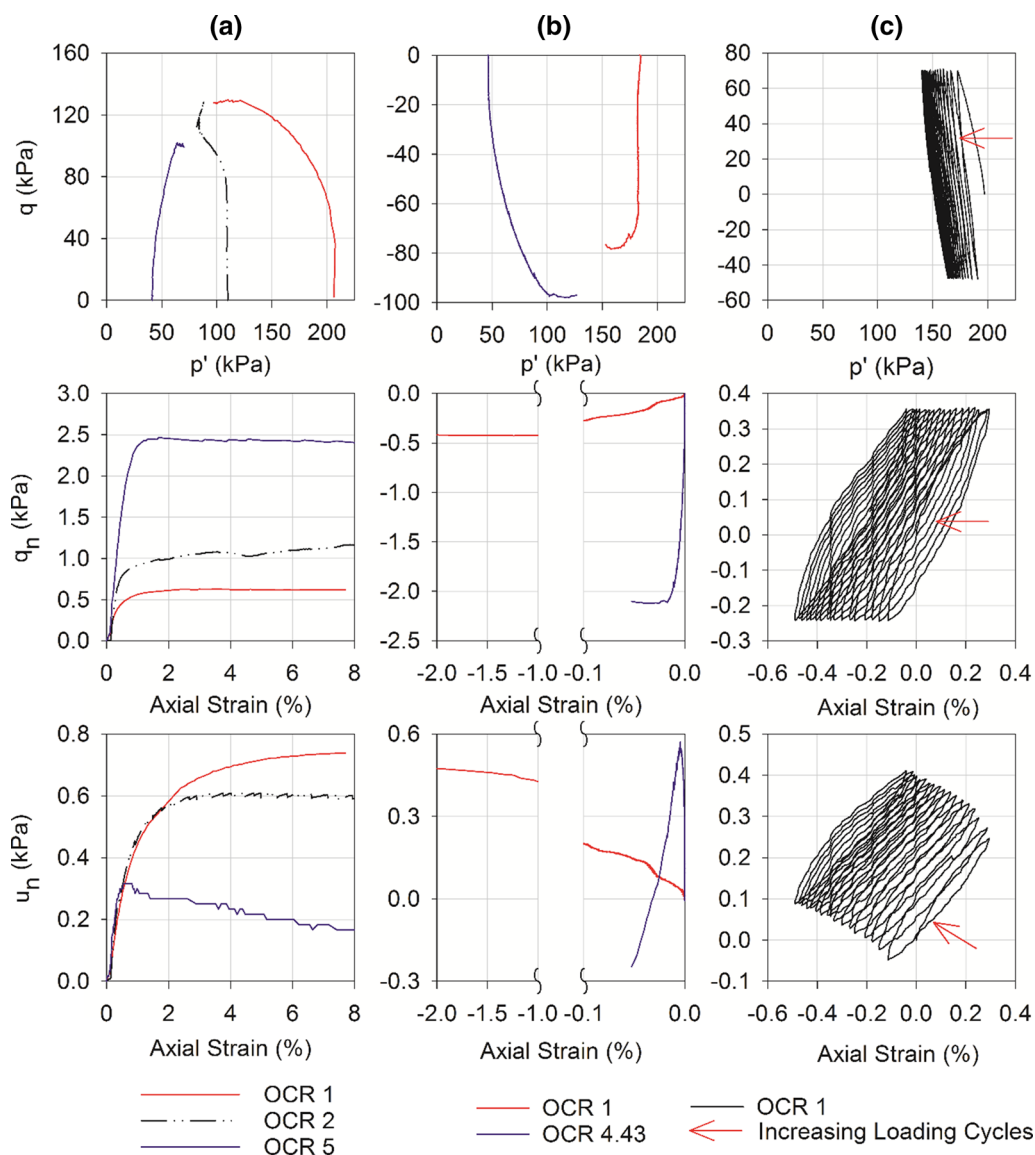


Fig. 6 Triaxial test results for unimproved natural clay: **a** CIUC tests; **b** CIUE tests; **c** CIU Cyclic test

specimens. Cyclic shear incorporated both compression and extension loading. Tests were run with a 1% per hour axial strain rate for unimproved soil and improved natural clay tests, and 4% per hour for the improved laboratory-created clay. Loading was reversed when the deviatoric stress reached a predetermined value, herein defined as the cyclic bounds. Tests on unimproved and improved laboratory-created, as well as unimproved natural, clay specimens used cyclic bounds equal to 60% of the deviatoric stress at failure of the respective normally consolidated CIUC or CIUE tests. Due to very large failure deviatoric stress and early onset of dilation for the improved natural clay in the normally consolidated CIUC test, the cyclic bound in compression was chosen as a value on the stress path prior to dilation in the normally consolidated CIUC

test. The cyclic bound in extension was set roughly equal to 55% of the bound in compression. Cyclic tests comprised of 20–40 cycles.

3 Laboratory test results

3.1 Oedometer tests

Oedometer test results for unimproved and improved tests are compared in Fig. 4. Schmertmann reconstruction was used to account for disturbance to the unimproved specimens. Recompression and virgin compression indices, for the unimproved soils, were calculated from the corrected oedometer results.

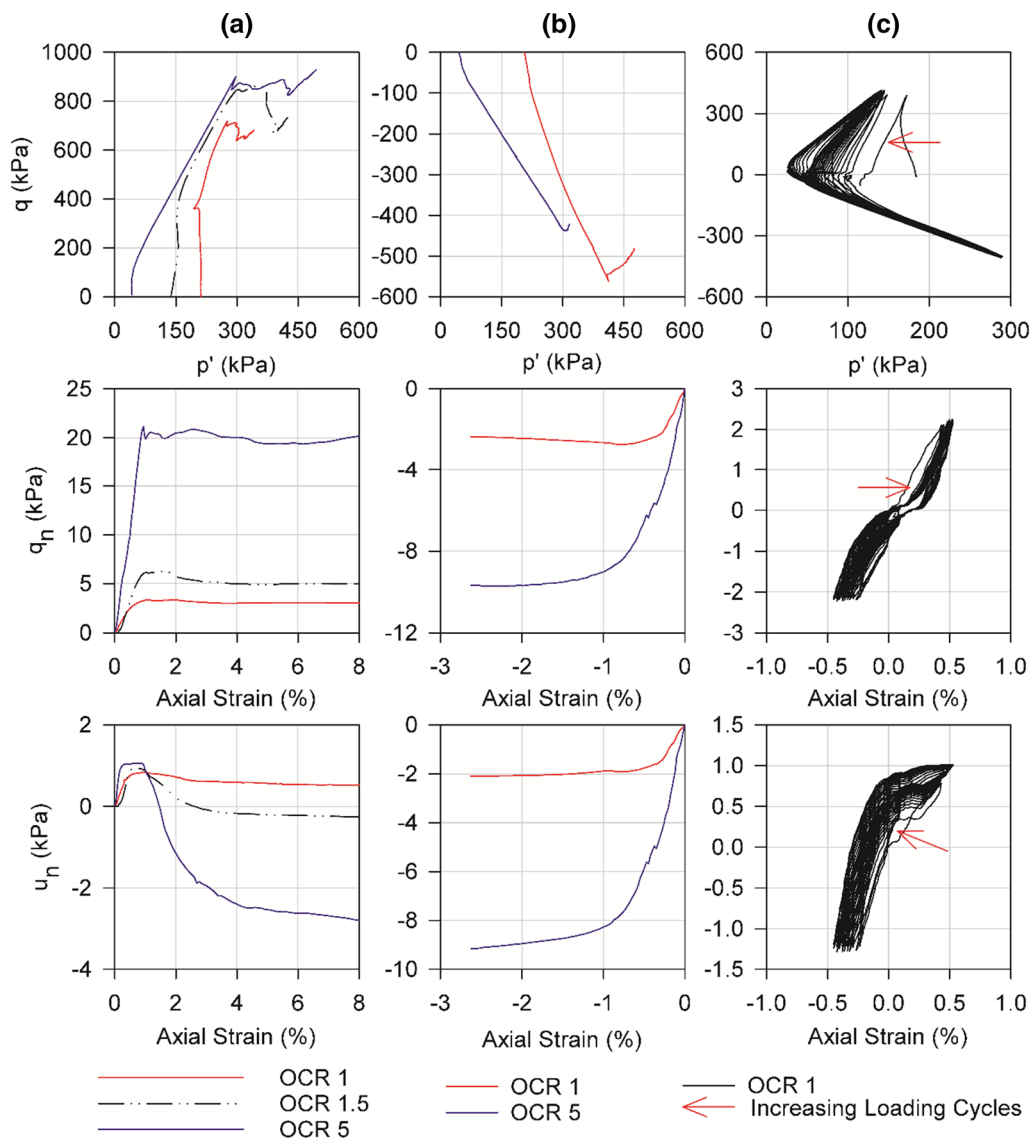


Fig. 7 Triaxial test results for improved laboratory-created clay: **a** CIUC tests; **b** CIUE tests; **c** CIU Cyclic test

Various compression indices for each specimen type are given in Table 4. Recompression indices were calculated from points on the unloading curves. The virgin compression sections for improved specimens are not clearly defined. Use of higher axial stresses may have resulted in a better defined linear virgin compression zone. Virgin compression indices for the improved soils were calculated through the final two points of the loading curve. Lorenzo and Bergado [30] showed that compression indices are often not drastically changed as a result of cement improvement: The recompression index may be reduced, but the virgin compression index is often increased due to the rapid breakdown of cementitious bonds after failure at higher stresses. However, in this research, the compression

indices for the laboratory-created clays changed drastically as a result of cement mixing. One may note that the unimproved laboratory-created clay specimen has a dramatically larger initial void ratio compared with the unimproved field and improved specimens due to the method of specimen creation. This drastic reduction in both the recompression and virgin compression indices may be in part due to the large discrepancy in initial void ratios.

The improved clay specimens have limited real stress history as a result of the specimen creation method; therefore, the approximately bilinear behavior is an effect of chemical bonding due to cement improvement. An *apparent preconsolidation pressure* can be obtained directly from the results using the Casagrande Method. Apparent

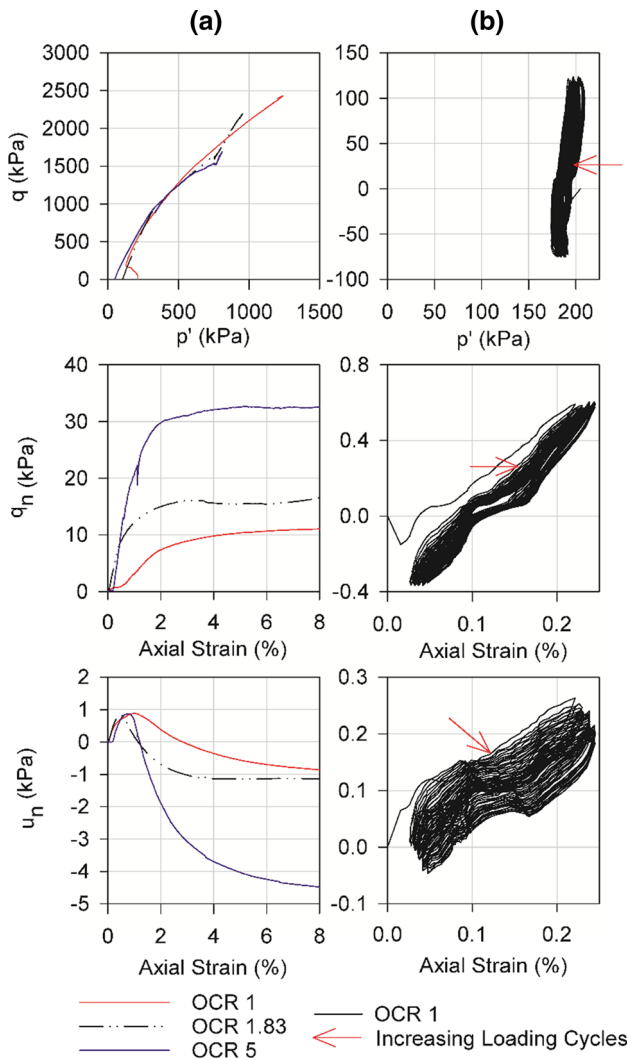


Fig. 8 Triaxial test results for improved natural clay: **a** CIUC tests; **b** CIU Cyclic test

preconsolidation pressures for the improved laboratory-created and natural clays were found to be 225 and 1500 kPa, respectively (see Fig. 4). A key aim of chemical improvement is increased stiffness. This increased stiffness is a result of the shift in the preconsolidation pressure and not a drastic change in individual compression indices. The results in Fig. 4 clearly show the axial strain incurred by both improved soil specimens is significantly lower than that of their respective unimproved specimens over the tested vertical stress range.

3.2 Triaxial tests

Triaxial test results are reported in Figs. 5, 6, 7 and 8. Imposed OCR values are also given in these figures. The mean effective stress (p') and deviatoric stress (q) are defined as:



Fig. 9 Typical modes of deformation of improved triaxial CIUC specimens following testing



Fig. 10 Typical modes of deformation of improved triaxial CIUE specimens following testing

$$p' = \frac{(\sigma'_1 + 2 \times \sigma'_3)}{3} \tag{5}$$

$$q = \sigma'_1 - \sigma'_3 \tag{6}$$

Division of the excess pore water pressure (u) and deviatoric stress by the final effective confining stress during consolidation results in the normalized generated pore water pressure (u_n) and normalized deviatoric stress (q_n). Triaxial test results for unimproved specimens, displayed

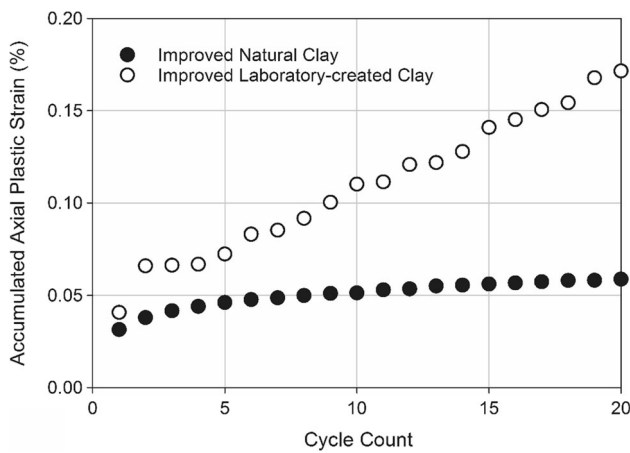


Fig. 11 Accumulation of axial plastic strain during cyclic loading of improved specimens

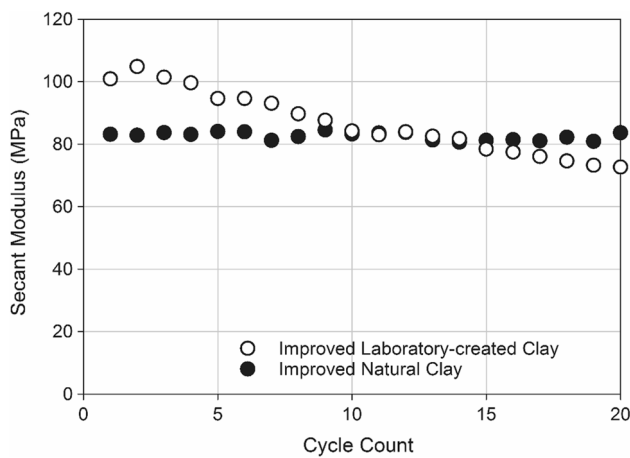


Fig. 12 Degradation of cyclic secant shear modulus during loading of improved specimens

in Figs. 5 and 6, agree with expected soft clay behavior. Trends associated with increased OCR: Increased normalized strength, increased normalized stiffness, and increased tendency for dilation during shear can be observed in both sets of data. Generation of positive pore water pressure, as measured during CIUE tests, is associated with the stress-controlled loading-type extension shear protocol chosen for this testing. CIU Cyclic results show gradual decrease in the amount of pore water pressure generated and axial strain accumulated per cycle as the number of loading cycles increase.

Results of the monotonic shear triaxial tests on improved specimens, Figs. 7a, b and 8a, exhibit stress-strain behaviors reminiscent of those of overconsolidated clays. All specimens sheared in compression show dilation and peak-residual strength behaviors. Extension shear tests of the laboratory-created improved clay exhibited negative excess pore water pressure generation due to the strain-controlled axial unloading extension shear protocol used

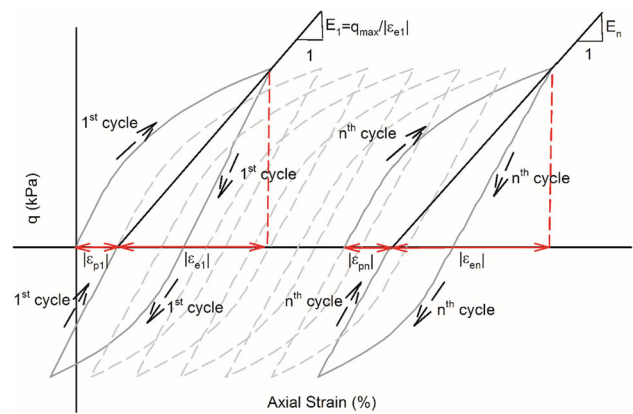


Fig. 13 Definition of cyclic degradation measures: axial plastic strain and cyclic secant shear modulus

Table 5 Bounding surface model parameters for unimproved clay

Model parameter	Laboratory-created clay	Natural clay
λ	0.140	0.104
κ	0.029	0.016
M_c	1.00	1.30
M_e/M_c	0.83	0.42
N	0.3	0.3
R_c	2.50	2.32
A_c	0.10	0.14
T	0.05	0.10
R_e/R_c	1.00	0.60
A_e/A_c	1.00	2.00
C	0.20	0.18
S	1.20	1.00
h_c	1.00	10.0
h_e/h_c	1.00	0.20
h_2	1.00	6.0

for testing. No CIUE tests were successfully completed using improved natural clay specimens due to axial loads in extension exceeding limitations of the testing apparatus. The presented results are in agreement with expectations of cement-mixed clay behavior discussed in the literature [36, 52, 59].

As far as the modes of deformations of the samples were concerned, improved CIUC specimens exhibited brittle behavior after reaching the peak stress that resulted in the formation of shear bands (see Fig. 9). CIUE specimens split along horizontal planes after reaching the peak stress (see Fig. 10). Unimproved specimens largely exhibited homogeneous deformation in compression and necking in extension.

Results of the CIU Cyclic tests for the improved specimens, Figs. 7c and 8b, show that equilibrium was reached

Table 6 Bounding surface model parameters for improved clay

Model parameter	Laboratory-created clay		Natural clay	
	Apparent preconsolidation pressure method	Fitted OCR method	Apparent preconsolidation pressure method	Fitted OCR method
λ	0.045	0.045	0.124	0.124
κ	0.0027	0.0027	0.0065	0.0065
M_c	3.00	3.00	2.325	2.325
M_e/M_c	0.47	0.47	0.20	0.20
N	0.3	0.3	0.3	0.3
R_c	1.30	2.00	1.30	2.30
A_c	0.03	0.10	0.03	0.05
T	0.05	0.05	0.05	0.05
R_e/R_c	0.4	1.00	1.00	1.00
A_e/A_c	0.6	1.00	1.00	1.00
C	0.20	0.00	0.15	0.10
S	1.00	1.00	1.00	1.80
h_c	85.0	200.0	85.0	10.0
h_e/h_c	0.18	1.00	1.00	1.00
h_2	50.15	200.0	85.0	10.0

within very few cycles although the number of cycles required to reach equilibrium is somewhat higher for the improved laboratory-created samples. The stresses imposed on the improved laboratory-created specimens were large enough for the stress path to follow the critical state line similar to what was seen in monotonic shear tests. On the other hand, the stresses used for CIU Cyclic improved natural clay testing were small compared to the ultimate strength of the specimen.

Following the guidance of Viana da Fonseca et al. [57], the accumulation of permanent axial strains and evolution of the secant modulus with cyclic loading are presented in Figs. 11 and 12, where the definitions of permanent strain and secant modulus are illustrated in Fig. 13. The improved natural clay specimen showed very little accumulation of plastic strain and no meaningful decrease in the secant modulus over the course of the test. Conversely, the improved laboratory-created clay specimen exhibited larger accumulation of plastic strains and an approximately 30% decrease in secant modulus. Viana da Fonseca et al. [57] stated that the decrease in the elastic modulus is directly related to the degradation of cementitious bonds; therefore, it can be inferred that the cyclic stress levels used for the improved natural clay were too small to cause degradation within 20 cycles. On the other hand, the cyclic stress levels used for the improved laboratory-created clay were sufficiently large to cause significant degradation. However, the results presented by Viana da Fonseca et al. [57] and Panico and Viana da Fonseca [35] suggest that even the cyclic loads imposed upon the improved natural clay specimen may be large enough to cause degradation of

the cementitious bonds given a suitable number of cycles (10,000+).

Comparisons of unimproved and improved clay results make clear the impact of the cement content on the stress–strain behavior.

- The initial tangent moduli for imposed OCR = 1 laboratory-created (10% cement) and natural (20% cement) improved specimens are, respectively, 4 times and 6 times greater than the moduli of their unimproved counterparts.
- The imposed OCR = 1 improved laboratory-created and improved natural specimens, respectively, failed at 8 and 19 times the deviatoric stress at failure of their unimproved counterparts.
- At similar confining stresses and OCR values, the change in compressive strength is approximately proportional to the cement content.
- Despite differing imposed OCR values, improved specimens of the same soil type have similar failure strengths and stiffness.

A more marked difference in stress–strain behavior can be observed between the different improved laboratory-created clay tests. However, as the initial effective confining stress prior to shear decreases, the improved laboratory-created clay CIUC stress path becomes increasingly similar to that of the improved natural specimens and the tendency toward dilation increases. The results for the improved natural clay specimens are ostensibly the same despite the difference in initial confining stress. It can be inferred that the influence of cementation predominates the

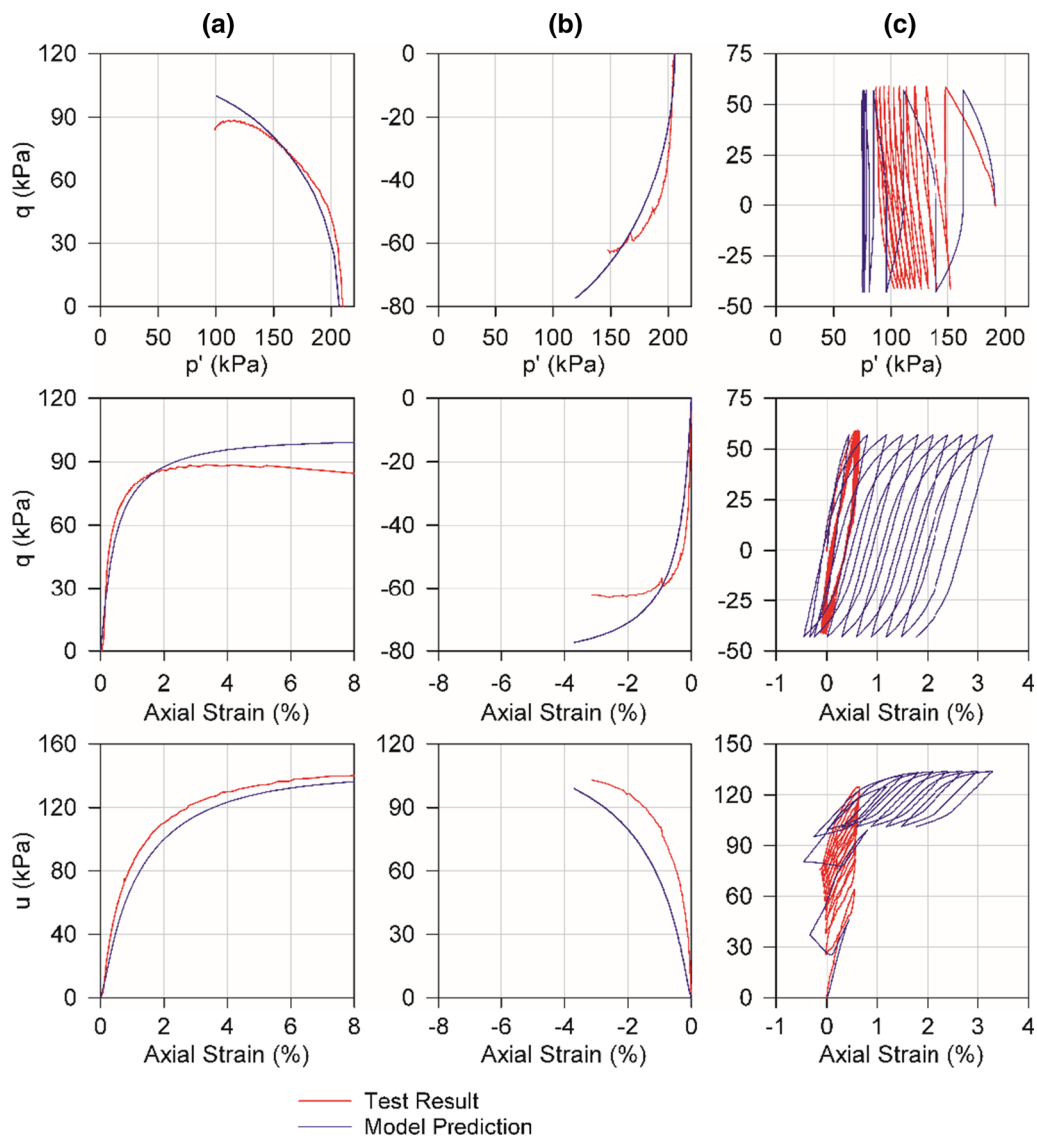


Fig. 14 Unimproved laboratory-created clay model comparisons: **a** CIUC OCR 1; **b** CIUE OCR 1; **c** CIU Cyclic OCR 1

stress–strain behavior over the influence of confining stress at relatively low consolidation/confining stress or high cement content.

From the laboratory testing results shown here, it is clear that the use of cement improvement can be used to increase soil strength and stiffness. Stress–strain behavior changes associated with cement improvement have been shown to be similar to changes that would occur from a substantial increase in the OCR.

4 Bounding surface elastoplastic model

Dafalias and Herrmann's [9] bounding surface elastoplastic model for clays uses 15 model parameters. The values of these parameters for unimproved and improved clays are

listed in Tables 5 and 6, respectively. Four of these parameters, the slopes of the recompression line (κ) and virgin compression line (λ) in e versus $\ln(p')$ space and the slopes of the critical state lines in compression (M_c) and extension (M_e) in p' versus q space, were directly obtained from oedometer and triaxial test results. The remaining parameters were calibrated using a systematic, and sequential, trial-and-error procedure outlined in Kaliakin et al. [16]. To begin, all parameters were set equal to the published typical values. Shape parameters, R_c and R_e , were calibrated by comparing model predictions with normally consolidated CIUC and CIUE results, respectively. Next, lightly overconsolidated specimen results were used to calibrate values for the projection center parameter, C , followed by hardening parameters, h_c , h_e , and h_2 . Finally, the elastic nucleus parameter, S_p , and shape

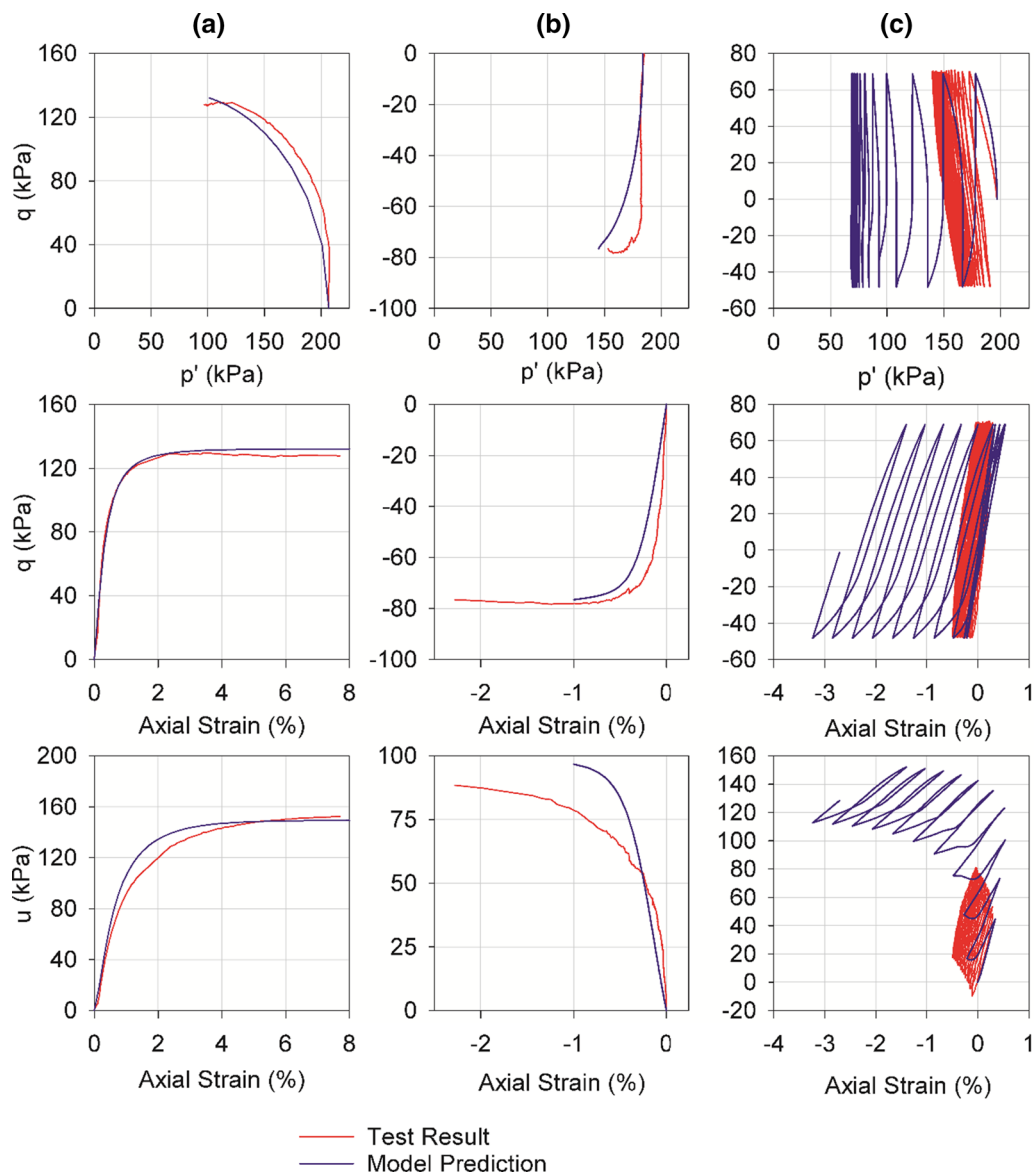


Fig. 15 Unimproved natural clay model comparisons: **a** CIUC OCR 1; **b** CIUE OCR 1; **c** CIU Cyclic OCR 1

parameters, A_c and A_e , were calibrated using heavily overconsolidated specimen results.

Comparisons of the model predictions and actual test results for both the unimproved laboratory-created and natural clays, in general, show reasonable agreement for the monotonic shear tests (Figs. 14, 15). Although not shown here, comparisons between predictions and test results for CIUC tests with other imposed OCR values are similar to those shown in Figs. 14 and 15. Predictions of CIU Cyclic results, with the exception of p' versus q behavior for laboratory-created specimen, show only little agreement with test results. Compression and extension loading have been demonstrated to be adequately predicted

by this model; therefore, shortcomings of this prediction are in the unloading phases. The bounding surface model assumes unloading to be elastic. It is possible that assuming elastoplastic unloading behavior will improve the predictions during cyclic loading.

The laboratory testing demonstrated that improved clay specimens share some stress–strain behaviors with overconsolidated clays. Artificial OCRs were defined for each test. In modeling, two methods of accounting for the effect of the artificial overconsolidation have been incorporated into the model calibrations and predictions. In the apparent preconsolidation pressure method, the values obtained from oedometer test results (see Fig. 4; Table 4) were

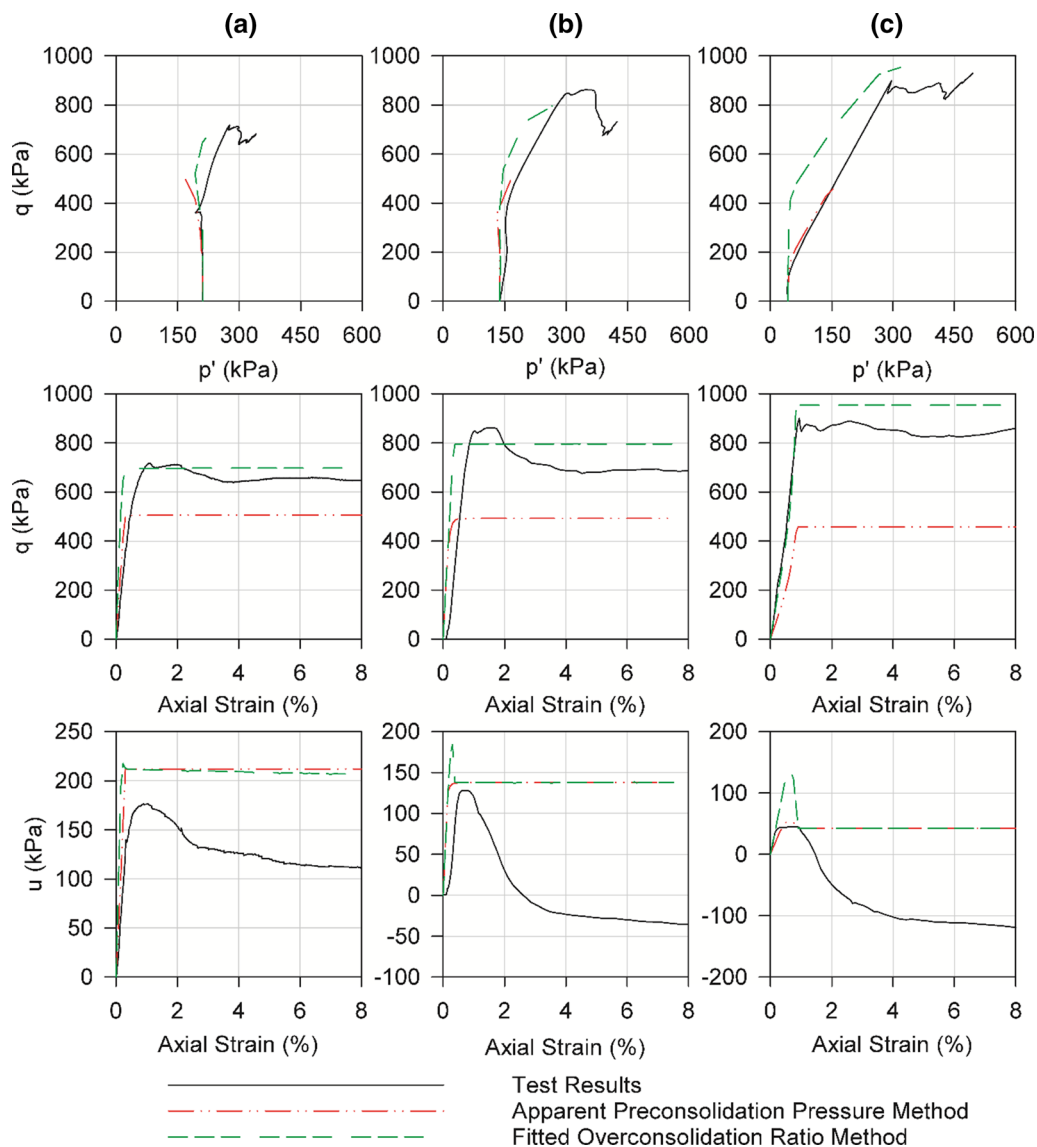


Fig. 16 Improved laboratory-created clay CIUC model comparisons: **a** Imposed OCR 1; **b** imposed OCR 1.5; **c** imposed OCR 5

directly used to define the OCR used in model predictions. The *fitted OCR* method of accounting for the artificial overconsolidation effect is to treat the OCR as an additional model parameter that requires calibration. After the 15 bounding surface model parameters were determined, OCRs were fitted by a trial-and-error method for each test. During this fitting, it was necessary to adjust some of the previously calibrated parameters.

Bounding surface model predictions resulting from both the apparent preconsolidation pressure method and fitted OCR method are compared with actual CIUC and CIUE triaxial test results in Figs. 16, 17, and 18. Overconsolidation ratios used in modeling are listed in Table 7. Each method of modeling improved specimen behavior showed some success in predicting the stress–strain behavior. Both

methods gave acceptable results for small-strain predictions of improved laboratory-created specimen tests. The fitted OCR method gave better predictions of final strength of CIUC results. The apparent preconsolidation pressure method was more accurate for CIUE predictions. Neither method was able to predict the stress–strain behavior of the improved natural clay specimens. Agreement can be noted in the p' versus q and ε_a versus u spaces; however, strength gain with axial strain is not accurately predicted. Failure strengths are predicted well by the fitted OCR method, by virtue of the fact that failure strength was a key parameter used in the calibration of the OCR in the fitted OCR method. Agreement between the apparent preconsolidation pressure method predictions and test results is the best when the imposed OCR is small.

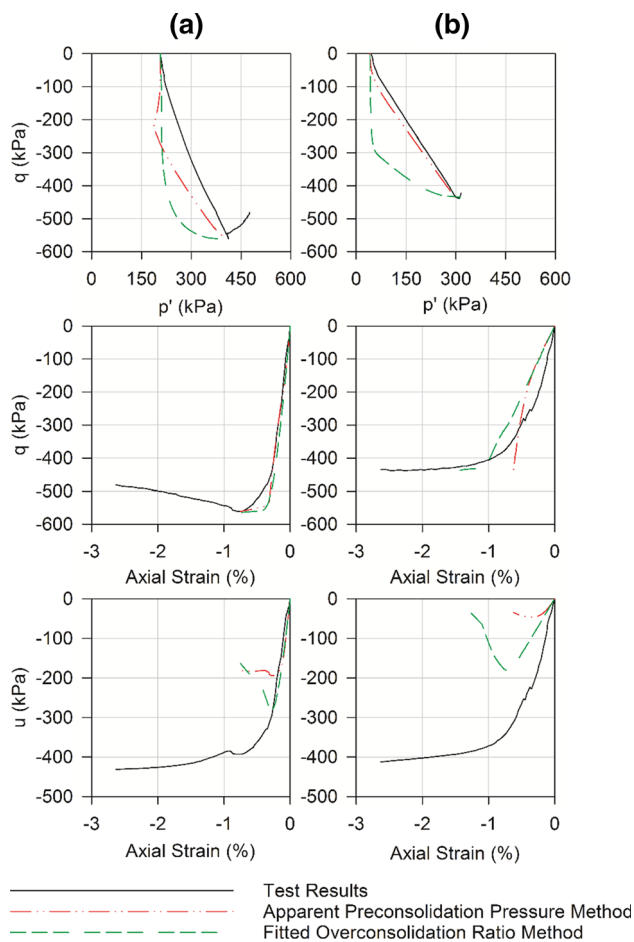


Fig. 17 Improved laboratory-created clay CIUE model comparisons: **a** Imposed OCR 1; **b** imposed OCR 5

Concave initial sections of the $\varepsilon_a - q$ predictions can be observed in all of the predictions for improved natural clay specimens and the CIUC and CIUE OCR 5 improved laboratory-created clay tests. A parametric study showed this concave behavior is due to larger critical state line slopes, M_c and M_e , than those normally associated with soft clays. The degree of the concavity increases as the artificial OCR increases.

It should be pointed out here that single element constitutive models are not appropriate to predict shear band formation and propagation in triaxial specimens. As shear bands were first observed at, or following, the peak shear stress in all improved triaxial test specimens, model predictions of the triaxial test results should not be expected to be an accurate representation of specimen behavior after the peak. Calibration of the model parameters, and the OCR in the fitted OCR method, was completed with consideration of only the stress–strain data at, and prior to, the occurrence of peak shear stress.

The bounding surface model used in this research has shown only limited potential for predicting the stress–strain

behavior of cement-improved clay triaxial specimens. With the introduction of a bonding parameter to describe the influence and degradation of the cementitious bonds in the specimen, as proposed by many researchers [e.g., 4, 7, 14, 18], the bounding surface model could better describe the stress–strain behavior of cement-improved clay soils. The behavior of cement-improved soils has been shown to change with the degradation of the bonds, theoretically, returning to the behavior of the unimproved soil after degradation of all cementitious bonds. The proposed bounding surface model can account for such changes by incorporating the new bonding parameter into the formulation of the yield surface and the changes in soil characteristics. As mentioned earlier, Taghavi [50], however, demonstrated that the level of accuracy in single element constitutive model predictions shown here may be sufficient to predict the macroscale behavior in boundary value problems, especially at small to moderate stresses far from failure.

5 Conclusions

The results of a series of laboratory tests on unimproved and improved specimens of two clay soils were presented. Laboratory testing results of both unimproved soils showed stress–strain behaviors in line with typical soft clay behavior. Improved specimens exhibited peak/residual behavior and dilation, as well as higher strength and stiffness over unimproved samples in triaxial compression. Depending on the cement content, the strength and stiffness could be improved from 8 to 19 times and 4 to 6 times, respectively.

The bounding surface elastoplastic model made reasonable predictions of the stress–strain behavior of unimproved clays under monotonic loading. Model predictions of CIU Cyclic test results were, however, not satisfactory. It is expected that making the unloading behavior elastoplastic in the model will improve the predictions for cyclic behavior. Two methods of accounting for the “artificial” stress history of improved soils for the bounding surface model predictions were detailed. The apparent preconsolidation pressure method is considerably easier to use, but the fitted OCR method gave better results over varied levels of confining stresses. The bounding surface model has limitations in predicting the stress–strain behavior for cement-improved clay, but can provide an approximation of the strength and stiffness with proper calibration. This investigation has demonstrated that the two modeling methods proposed give the best predictions when the artificial OCR is small, which corresponds to smaller cement contents.

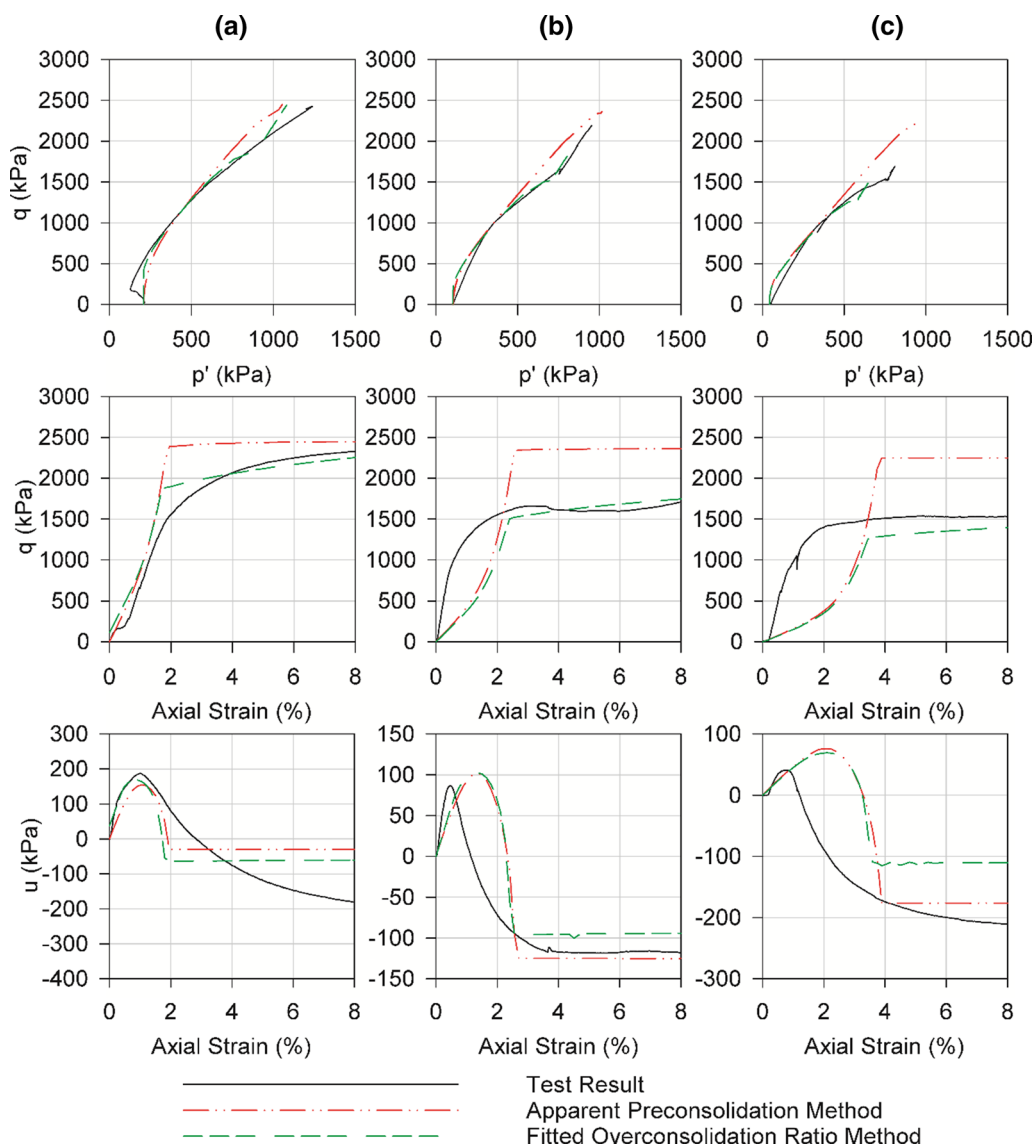


Fig. 18 Improved natural clay CIUC model comparisons: **a** Imposed OCR 1; **b** imposed OCR 1.83; **c** imposed OCR 5

Table 7 Overconsolidation ratios used in improved clay predictions

	Test type	Imposed OCR	Bounding surface model	
			Apparent preconsolidation pressure method	Fitted OCR method
Laboratory clay	CIUC	1.0	1.06	2.25
	CIUC	1.5	1.63	4.00
	CIUC	5.0	5.29	17.0
	CIUE	1.0	1.09	4.0
	CIUE	5.0	5.49	17.0
Natural clay	CIUC	1.0	7.27	14.4
	CIUC	1.83	13.3	21.8
	CIUC	5.0	36.3	43.5

Acknowledgements This project was funded by a U.S. National Science Foundation (NSF) George E. Brown, Jr. Network for Earthquake Engineering Simulation Research (NEESR) Grant (Grant No. CMMI-0830328). The first author was also funded by two fellowships from NSF (through Grant Nos. HRD-1249206 and HRD-0902027). This support from NSF is gratefully acknowledged. Any opinions, findings, and conclusions or recommendations expressed in this paper are those of the authors and do not necessarily reflect the views of NSF. Hoda Soltani’s contribution to some of the laboratory tests presented in this paper is also acknowledged.

References

1. Abu-Farsakh M, Dhakal S, Chen Q (2015) Laboratory characterization of cementitiously treated/stabilized very weak subgrade soil under cyclic loading. *Soils Found* 55(3):504–516

2. Ahnberg H (2007) On yield stresses and the influence of curing stresses on stress paths and strength measured in triaxial testing of stabilized soils. *Can Geotech J* 44:54–66. doi:[10.1139/t06-096](https://doi.org/10.1139/t06-096)
3. Andromalos K, Hegaxy Y, Jasperse B (2001) Stabilization of soft soils by soil mixing. In: *Soft ground technology (GSP 112)*, pp 194–205. doi:[10.1061/40552\(301\)16](https://doi.org/10.1061/40552(301)16)
4. Arroyo M, Ciantia M, Castellanza R, Gens A, Nova R (2012) Simulation of cement-improved clay structures with a bonded elasto-plastic model: a practical approach. *Comput Geotech* 45:140–150
5. Arroyo M, Castellanza MC, Gens A (2011) A soft-rock model for cement-improved clays. In: *15th European conference of soil mechanics and foundation engineering*, pp 501–506
6. Asaoka A, Nakano M, Nora T (2000) Superloading yield surface concept for highly structured soil behaviour. *Soils Found* 40(2):99–110
7. Baudet B, Stallebrass S (2004) A constitutive model for saturated clays. *Géotechnique* 54(4):269–278
8. Bruce MEC, Berg RR, Collin JG, Filz GM, Terashi M, Yang DS (2013) Federal Highway Administration design manual: deep mixing for embankment and foundation support, Report No. FHWA-HRT-13-046. Federal Highway Administration, Washington
9. Dafalias YF, Herrmann LR (1986) Bounding surface plasticity II: application to isotropic cohesive soils. *J Eng Mech* 112(12):1263–1291. doi:[10.1061/\(ASCE\)0733-9399\(1986\)112:12\(1263\)](https://doi.org/10.1061/(ASCE)0733-9399(1986)112:12(1263))
10. Filz GM, Hodges DE, Weatherby DE, Marr WA (2005) Standardized definitions and laboratory procedures for soil–cement specimens applicable to the wet method of deep mixing. In: *Innov grouting soil improv (GSP 136)*, pp 1–13. doi:[10.1061/40783\(162\)1](https://doi.org/10.1061/40783(162)1)
11. Fleming BJ, Sritharan S, Miller GA, Muraleetharan KK (2016) Full-scale seismic testing of piles in improved and unimproved soft clay. *Earthq Spectra* 32(1):239–265. doi:[10.1193/012714EQS018M](https://doi.org/10.1193/012714EQS018M)
12. Gonzalez NA, Gens A, Arroyo M, Rouainia M (2011) A structured constitutive model for simulating the behaviour of an overconsolidated bonded clay. In: *9th international conference on computational plasticity, fundamentals and applications*, pp 2–12
13. Hodges DK, Filz GM, Weatherby DE (2008) Laboratory mixing, curing, and strength testing of soil–cement specimens applicable to the wet method of deep mixing, CGPR Report No. 48. Virginia Tech Center for Geotechnical Practice and Research, Blacksburg, Virginia
14. Horpibulsuk S, Liu MD, Liyanapathirana DS, Suebsuk J (2010) Behaviour of cemented clay simulated via the theoretical framework of the structured Cam clay model. *Comput Geotech* 37:1–9
15. Japanese Geotechnical Society (2000) Practice for making and curing stabilized soil specimens without compaction, JGS T 0821-2000. Japanese Geotechnical Society, Tokyo
16. Kaliakin VN, Dafalias YF, Herrmann LR (1987) Time dependent bounding surface model for isotropic cohesive soils: notes for a short course. In: *Second International Conference on Constitutive Laws for Engineering Materials: THEORY and APPLICATION*, Tucson, Arizona
17. Kamruzzaman AHM, Chew SH, Lee FH (2009) Structuration and destructuration behavior of cement-treated Singapore marine clay. *J Geotech Geoenviron Eng* 135:573–589. doi:[10.1061/\(ASCE\)1090-0241\(2009\)135:4\(573\)](https://doi.org/10.1061/(ASCE)1090-0241(2009)135:4(573))
18. Kasama K, Ochiai H, Yasufuku N (2000) On the stress–strain behaviour of lightly cemented clay based on an extended critical state concept. *Soils Found* 40(5):37–47
19. Kavvasdas M, Amorosi A (2000) A constitutive model for structured soils. *Géotechnique* 50(3):263–273
20. Kirupakaran K, Cerato AB, Liu C, Miller GA, Muraleetharan KK, Pinilla JD, Price S, Thompson ZM (2010) Simulation of a centrifuge model test of pile foundations in CDSM improved soft clays. In: *GeoFlorida 2010: adv anal, model des (GSP 199)*, pp 1583–1591
21. Lapointe E, Fannin J, Wilson B (2012) Cement-treated soil: variation of UCS with soil type. In: *Grouting deep mixing 2012 (GSP 228)*, pp 512–521. doi:[10.1061/9780784412350.0037](https://doi.org/10.1061/9780784412350.0037)
22. Lee K, Chan D, Lam K (2004) Constitutive model for cement treated clay in a critical state framework. *Soils Found* 44(3):69–77
23. Lee KH, Lee S (2002) Mechanical Properties of Weakly Bonded Cement Stabilized Kaolin. *KSCE J Civ Eng* 6(4):389–398. doi:[10.1007/BF02841993](https://doi.org/10.1007/BF02841993)
24. Liu MD, Carter JP (2000) Modelling the destructuring of soils during virgin compression. *Géotechnique* 50(4):479–483
25. Liu C, Soltani H, Muraleetharan KK, Cerato AB, Miller GA, Sritharan S (2016) Cyclic and seismic response of single piles in improved and unimproved soft clays. *Acta Geotech* 11:1431–1444. doi:[10.1007/s11440-016-0504-2](https://doi.org/10.1007/s11440-016-0504-2)
26. Liu C, Soltani H, Pinilla JD, Muraleetharan KK, Cerato AB, Miller GA (2011) Centrifuge investigation of seismic behavior of pile foundations in soft clays. *Geo-Frontiers 2011:585–594*. doi:[10.1061/41165\(397\)61](https://doi.org/10.1061/41165(397)61)
27. Liu MD, Carter JP, Horpibulsuk S, Liyanapathirana DS (2006) Modelling the behavior of cemented clay. In: *Ground modif seism mitig (GSP 152)*, pp 65–72
28. Liu C, Soltani H, Muraleetharan K, Cerato C, Miller GA, Sritharan S (2014) Cyclic loading of single piles—centrifuge model No. 1. Network for earthquake engineering simulation (distributor), Dataset. doi:[10.4231/D3S46H66Q](https://doi.org/10.4231/D3S46H66Q)
29. Liu C, Soltani H, Muraleetharan K, Cerato A, Miller GA, Sritharan S (2014) Dynamic loading of single piles—centrifuge model No. 2. Network for earthquake engineering simulation (distributor), Dataset. doi:[10.4231/D31N7XN5R](https://doi.org/10.4231/D31N7XN5R)
30. Lorenzo GA, Bergado DT (2004) Fundamental parameters of cement-admixed clay—new Approach. *J Geotech Geoenviron Eng* 130:1042–1050. doi:[10.1061/\(ASCE\)1090-0241\(2004\)130:10\(1042\)](https://doi.org/10.1061/(ASCE)1090-0241(2004)130:10(1042))
31. Miura N, Horpibulsuk S, Nagaraj TS (2001) Engineering behavior of cement stabilized clay at high water content. *Soils Found* 45(5):33–45
32. Muraleetharan KK, Ravichandran N, Taylor LM (2003) TeraDysac: TeraScale dynamic soil analysis code. Computer Code, School of Civil Engineering and Environmental Science, University of Oklahoma, Norman
33. Nguyen LD, Fatahi B, Khabbaz H (2014) A constitutive model for cemented clays capturing cementation degradation. *Int J Plast* 56:1–18
34. Nova R, Castellanza R, Tamagnini C (2003) A constitutive model for bonded geomaterials subject to mechanical and/or chemical degradation. *Int J Numer Anal Methods Geomech* 27(9):705–732
35. Panico F, Viana da Fonseca A (2016) Long term cyclic response of a soil–cement mixture: experimental study and modelling. *Procedia Eng* 143:178–186. doi:[10.1016/j.proeng.2016.06.023](https://doi.org/10.1016/j.proeng.2016.06.023)
36. Porbaha A, Shibuya S, Kishida T (2000) State of the art in deep mixing technology. Part III: geomaterial characterization. *Ground Improv* 4(3):91–110. doi:[10.1680/grim.2000.4.3.91](https://doi.org/10.1680/grim.2000.4.3.91)
37. Porbaha A, Tanaka H, Kobayashi M (1998) State of the art in deep mixing technology: part II. Applications. *Ground Improv* 2(3):125–139. doi:[10.1680/gi.1998.020303](https://doi.org/10.1680/gi.1998.020303)
38. Porbaha AA (2006) Recent advances in deep mixing research and development in the USA. In: *Ground modif seism mitig (GSP 152)*, pp 45–50. doi:[10.1061/40864\(196\)7](https://doi.org/10.1061/40864(196)7)
39. Quiroga AJ (2013) Modeling of pile foundations in unimproved and cement-improved soft clays: laboratory testing and field validation. Thesis, University of Oklahoma

40. Ravichandran N (2005) A framework-based finite element approach for solving large deformation problems in multi-phase porous media. Dissertation, School of Civil Engineering and Environmental Science, University of Oklahoma
41. Rouainia M, Muir Wood D (2000) A kinematic hardening constitutive model for natural clays with loss of structure. *Géotechnique* 50(2):153–164
42. Sheeran DE, Krizek RJ (1971) Preparation of homogeneous soil samples by slurry consolidation. *J Mater* 6(2):356–373
43. Shen S, Xu Y, Han J, Zhang J (2012) A ten-year review on the development of soil mixing technologies in China. In: *Grouting deep mixing 2012 (GSP 228)*, pp 343–356. doi:[10.1061/9780784412350.0020](https://doi.org/10.1061/9780784412350.0020)
44. Shrestha R, Al-Tabbaa A (2012) Development of predictive models for cement stabilized soils. In: *Grouting deep mixing 2012 (GSP 228)*, pp 221–230. doi:[10.1061/9780784412350.0008](https://doi.org/10.1061/9780784412350.0008)
45. Suebsuk J, Horpibulsuk S, Liu MD (2010) Modified structured Cam clay: a generalized critical state model for destructured, naturally structured and artificially structured clays. *Comput Geotech* 37:956–968
46. Suebsuk J, Horpibulsuk S, Liu MD (2011) A critical state model for overconsolidated structured clays. *Comput Geotech* 38:648–658
47. Taghavi A, Miller G, Muraleetharan K (2010) NEES-pilEs full-scale field testing in Miami, Oklahoma: geotechnical site investigation report, technical report. School of Civil Engineering and Environmental Science, University of Oklahoma, Norman
48. Taghavi A, Muraleetharan KK, Miller GA, Cerato AB (2016) Centrifuge modeling of laterally loaded pile groups in improved soft clay. *J Geotech Geoenviron Eng* 142(4):1–13. doi:[10.1061/\(ASCE\)GT.1943-5606.0001443](https://doi.org/10.1061/(ASCE)GT.1943-5606.0001443)
49. Taghavi A, Muraleetharan K, Miller G, Cerato A (2013) Seismic and cyclic lateral load tests of pile groups and single piles—centrifuge model No. 4. Network for earthquake engineering simulation (distributor), Dataset. doi:[10.4231/D39P2W61H](https://doi.org/10.4231/D39P2W61H)
50. Taghavi A (2015) Seismic and quasi-static lateral load behavior of groups in improved soft clay: centrifuge and numerical modeling. Dissertation, University of Oklahoma
51. Taiebat M, Dafalias YF, Peek R (2010) A destructure theory and its application to SANICLAY model. *Int J Numer Anal Methods Geomech* 34:1009–1040
52. Tatsuoka F, Kobayashi A (1983) Triaxial strength characteristics of cement-treated soft clay. In: *Proceedings of the 8th European conference of SMFE*, pp 421–426
53. Thompson ZM (2011) Stress–Strain behavior of unimproved and cement-improved soft clays. Thesis, University of Oklahoma
54. Uddin K, Balasubramaniam AS, Bergado DT (1997) Engineering behavior of cement-treated Bangkok soft clay. *Geotech Eng* 28(1):89–119
55. Upadhyaya S, Tiwari B, Olgun G (2016) Static and dynamic properties of compacted soil–cement mixtures. *Geotech Struct Eng Congr 2016*:1646–1654
56. Vatsula A, Nova R, Srinivasa M (2001) Elastoplastic model for cemented soils. *J Geotech Geoenviron Eng* 127(8):679–687
57. Viana da Fonseca A, Rios S, Amaral MF, Panico F (2013) Fatigue cyclic tests on artificially cemented soil. *Geotech Test J* 36(2):227–235. doi:[10.1520/GTJ20120113](https://doi.org/10.1520/GTJ20120113)
58. Xiao H, Lee FH, Liu Y (2016) Bounding surface Cam-clay model with cohesion for cement-admixed clay. *Int J Geomech* 17:04016026
59. Yin JH (2001) Stress–strain–strength characteristics of soft Hong Kong marine deposits without or with cement treatment. *Lowl Technol Inst* 3(1):1–13